

Highly Sensitive, Printable Nanostructured Conductive Polymer Wireless Sensor for Food Spoilage Detection

Zhong Ma,^{†,‡} Ping Chen,[†] Wen Cheng,[†] Kun Yan,[†] Lijia Pan,^{*,†} Yi Shi,^{*,†} and Guihua Yu^{*,‡}

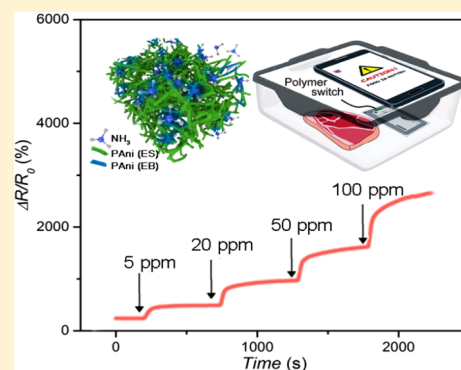
[†]Collaborative Innovation Center of Advanced Microstructures, Jiangsu Provincial Key Laboratory of Photonic and Electronic Materials, School of Electronic Science and Engineering, Nanjing University, 210093 Nanjing, China

[‡]Materials Science and Engineering Program and Department of Mechanical Engineering, The University of Texas at Austin, Austin, Texas 78712, United States

Supporting Information

ABSTRACT: Near-field communication (NFC) labeling technology has been recently used to endow smartphones with nonline-of-sight sensing functions to improve the environment, human health, and quality of life. For applications in detecting food spoilage, the development of a sensor with high enough sensitivity to act as a switch for an NFC tag remains a challenge. In this Letter, we developed a nanostructured conductive polymer-based gas sensor with high sensitivity of $\Delta R/R_0 = 225\%$ toward 5 ppm ammonia NH_3 and unprecedented sensitivities of 46% and 17% toward 5 ppm putrescine and cadaverine, respectively. The gas sensor plays a critical role as a sensitive switch in the circuit of the NFC tag and enables a smartphone to readout meat spoilage when the concentration of biogenic amines is over a preset threshold. We envision the broad potential use of such intelligent sensing for food status monitoring applications in daily life, storage and supply chains.

KEYWORDS: Wireless sensor, food spoilage, polyaniline, nanostructured polymer, gas sensors



Recently, the application of near field communication (NFC) technology in wireless intelligent devices was reported due to their portable, low-cost, battery-free and smartphone-communicable features.^{1,2} An NFC tag is an inexpensive and convenient paper-like resonant circuit that can be easily placed anywhere, allowing contactless communication with a smartphone to transfer stored information once the tag is detected to be readable. On the basis of these advantages, the NFC tag can be equipped with additional sensing abilities by modification with a sensor to switch the smartphone readout upon contacting a certain amount of a chemical.³

A precise, convenient, and low-cost method to assess the status of food is highly desired to help avoid spoilage for consumers, storage, and supply chains. Analytical methods for monitoring meat spoilage rely on the detection of the total volatile basic nitrogen (TVBN), including biogenic amines (BAs) and ammonia (NH_3).⁴ Among them, BAs, such as putrescine and cadaverine, are the most significant markers and the origin of the bad odor from meat decomposition; these molecules are mainly formed through the decarboxylation of amino acids under interaction with microbes.^{5,6} However, the detection of BAs still relies on conventional methods, such as chromatography,⁷ electrochemistry,⁸ chemiluminescence,⁹ and spectrometry,¹⁰ which suffer from the shortcomings of bulky and expensive equipment, poor portability, and complex sample processing. An alternative method for the determination of biogenic amines in foods is the use of chemiresistive gas sensors.¹¹ However, the realization of a high-sensitivity BA

sensor using nontoxic material still remains a challenge, because the BA concentrations in spoiled food are relatively low (ranging from 2 to 1500 $\text{mg} \cdot (100 \text{ g})^{-1}$ putrescine and cadaverine in different meat samples,⁴ that is, 5–8 ppm at the stage of initial decomposition with storage for 5 days at 5 °C and 17–186 ppm at the stage of advanced decomposition with storage for 7 days at 5 °C).^{12,13} The relationship between amine concentration within meat samples and vapor phase concentration (ppm) is in accordance to Raoult's Law (Supporting Information). These drawbacks impede consumers from precisely and conveniently assessing the status of a food at low cost.

In this research, we aim to incorporate NFC tags with a sensitive switch to detect food spoilage with a smartphone. As an important parameter to determine the readability of the NFC tag, the change in the reflection coefficient (S_{11}) corresponds to the switchability of the tag.¹⁴ NFC tags have been considered as a powerful platform for wireless sensing, yet current detection methods still rely on expensive, professional microwave network analyzers due to the difficulty in switching NFC tags between on and off states.^{2,15} An ideal switch needs to have a large On–Off ratio of S_{11} , that is, high sensitivity, to transform the TVBN concentration information into a large variation in the complex impedance of the tag.

Received: May 4, 2018

Revised: June 2, 2018

Herein we developed a nanostructured conductive polymer-based gas sensor that can detect various TVBN concentrations with very high sensitivities $\Delta R/R_0$ of 225%, 46%, and 17% toward 5 ppm of NH_3 , putrescine, and cadaverine, respectively. The conductive polymer itself and the dopant are nontoxic. Furthermore, the sensing material was printed on the NFC tag. The gas sensor with a high On–Off ratio plays the role as a sensitive switch in the circuit of the NFC tag, enabling the smartphone to readout meat spoilage when the concentration of biogenic amines is over a preset threshold (Figure 1). This

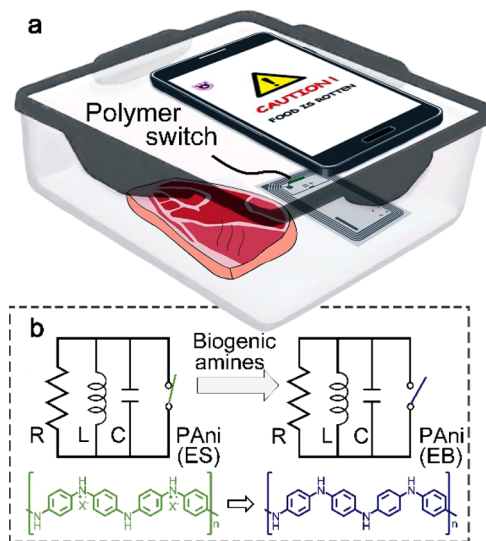


Figure 1. Schematic illustration of the wireless badge for food spoilage detection. (a) PTS–PAni is exploited as a conductive polymer switch to modify an NFC tag to detect food spoilage. (b) The circuit of the modified NFC tag. The amine gas released from spoiled meat dedopes PTS–PAni and increases the resistance of the device and thus switches the readability of the NFC tag.

intelligent sensing device realizes an effective wireless sensing assisted by mobile phones without requiring professional equipment and shows tremendous promise in applications for food status monitoring in daily life.

As schematically illustrated in Figures 1b and 2a, nanostructured polyaniline (PAni) is an ideal switch material because PAni undergoes large changes in its electric properties upon gas-phase doping/dedoping interactions with amines.^{16–18} In this study, we found that iron(III) p-toluene sulfonate hexahydrate-doped PAni shows very high sensitivity as an amine-sensing material. PAni itself is nontoxic and has excellent *in vitro* and *in vivo* biocompatibility, according to previous research.^{19–21} PAni is easy to be micropatterned on an NFC tag by inkjet printing technology (Figure 2d).¹⁶ We chose p-toluene sulfonate hexahydrate (PTS) (Figure 2b) and PTS is permitted to be used in food additives according to regulations of the United States Food and Drug Administration (FDA)²² and because its sulfonate functional group can dope PAni efficiently. The iron(III) ion acts as the initiator of aniline polymerization and excessive ions were removed in the purification process. Figure 2c shows the Fourier transform infrared (FT-IR) spectra of PTS-doped PAni (PTS–PAni). The bands at 1560 and 1487 cm^{-1} are attributed to C=N and C=C stretching mode of vibration for the quinonoid and benzenoid units of PAni; 1298 and 1240 cm^{-1} are stretching peaks of C–N for benzenoid units. 1031 cm^{-1} is stretching peak of p-toluene sulfonic acid group. The scanning electron microscope (SEM) and transmission electron microscope (TEM) images show the morphology of PTS–PAni to have a foam-like structure constructed from interconnected nanofibers with diameters of approximately 60 nm (Figure 2e,f and Supporting Information Figure S1).^{23–25} The morphology of the interconnected nanofibers offers a more efficient surface-to-volume ratio than bulky materials, facilitates electron transport and provides more active sites for gas adsorption

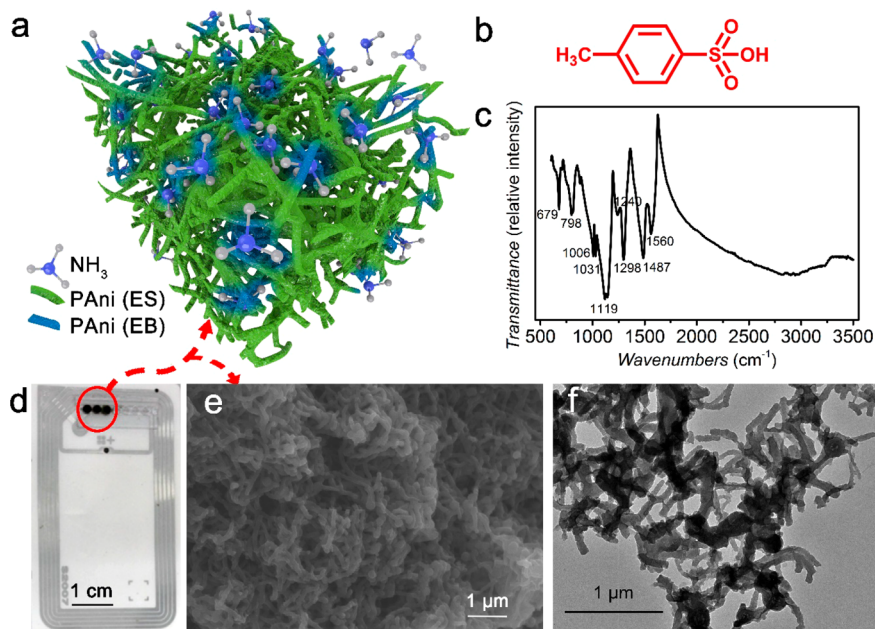


Figure 2. Characterization of PTS–PAni. (a) Schematic illustration of the general sensing mechanism of PTS–PAni. The color change of PTS–PAni from green to blue indicates that PAni is dedoped into insulating emeraldine base (EB) form from its conductive emeraldine salt (ES) form upon interacting with amine gas. (b) Chemical structure of PTS. (c) FT-IR spectra of PTS–PAni. (d) Photograph of an NFC tag modified with printed PTS–PAni. (e,f) SEM and TEM images of PTS–PAni, respectively.

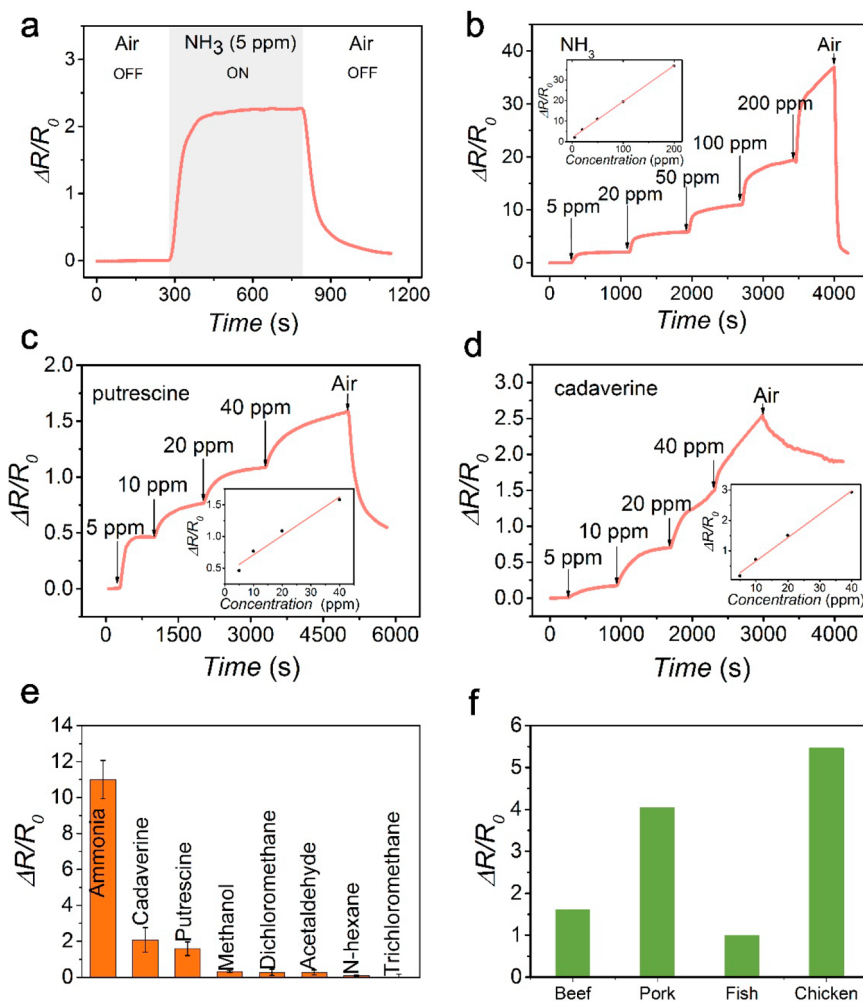


Figure 3. Sensing performances of PTS-PANI. (a) Response of PTS-PANI to 5 ppm of NH₃. (b) Dynamic responses of PTS-PANI to different concentrations of NH₃. (c) Dynamic responses of PTS-PANI to different concentrations of putrescine. (d) Dynamic responses of PTS-PANI to different concentrations of cadaverine. (e) Selectivity of PTS-PANI to different volatile solvents. (f) Responses of PTS-PANI to four kinds of raw meats, that is, beef, pork, fish, and chicken. The weight of each meat sample is 20 g, and the meats were stored at 30 °C for 20 h.

(Figure 2a). The conductivity of PTS-PANI was measured to be 16 S·m⁻¹ by the standard four-probe method.

The porous nanostructure of PTS-PANI, with larger surface area and smaller diameter, allows a sensitive response to amines. Herein, the sensitivity is defined as

$$S = \frac{\Delta R}{R_0} = \frac{R_g - R_0}{R_0} \quad (1)$$

where R_0 and R_g represent the resistance of the PANi film before and after exposure to NH₃ gas, respectively. As shown as Figure 3a, an immediate increase in resistance was observed as soon as PTS-PANI was exposed to 5 ppm of NH₃. The color change of nanofibers in Figure 2a indicates that PTS-PANI is dedoped into its emeraldine base (EB) form (insulating state) from its emeraldine salt (ES) form by interaction with base gas, as shown in Figure 1b.^{26,27} The sensitivity was measured to be as high as 225% (45% change in the resistance per ppm) with a response time of approximately 112 s. PTS-PANI provides an excellent dynamic response to NH₃ in a wide range of concentrations, as shown as Figure 3b. An linear increase in the resistive response was observed with increasing concentration of NH₃ gas (inset in Figure 3b) and the sensitivity is among those of the best reported NH₃ sensors

(Supporting Information Table S1).^{28,29} The resistance of PANi approaches its original baseline level upon exposure to air, suggesting the excellent reversibility of the sensor, which is also demonstrated in Supporting Information Figure S2.

PTS-PANI exhibited high sensitivity toward BAs, which is the key factor to identify spoiled food.^{5,6} As shown in Figure 3c,d, PTS-PANI achieved an unprecedented sensitivity of 46% toward 5 ppm putrescine (9.20% change in the resistance per ppm) and 17% toward 5 ppm cadaverine (4.25% change in the resistance per ppm) at room temperature. As implied by its sensing mechanism, PTS-PANI should be able to respond to all kind of BAs.

The PTS-PANI exhibits a large response only to TVBN, while its response to other volatile solvents is negligible (Figure 3e). This selectivity may be attributed to the fact that amines are reducing agents, which can donate a lone electron to PTS-PANI and result in significant dedoping and increase the resistance of PANi.³⁰ To illustrate the capability of our sensors to detect food spoilage, we employed PTS-PANI to detect the spoilage of common meat products stored at 30 °C for 20 h (pork, beef, chicken, and fish). Even the lowest $\Delta R/R_0$ is as high as 100% for the sensor interacting with the odor of fish and can be as high as 500% for the sensor detecting the odor of

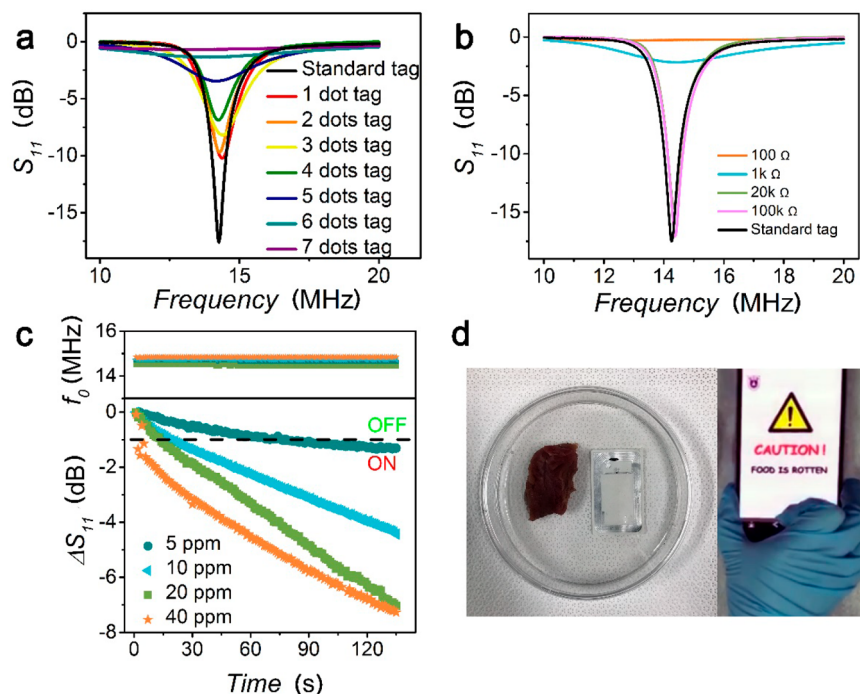


Figure 4. Application of a wireless badge in food spoilage detection. (a) S_{11} -frequency traces of NFC tags modified with different amounts of PTS-PAni. (b) S_{11} -frequency traces of tags modified with fixed-value resistors. (c) The real-time responses in S_{11} and f_0 toward 5, 10, 20, and 40 ppm of NH_3 . (d) Application of modified NFC tags in using a smartphone to detect meat spoilage.

chicken, indicating that the gas sensor will work as a sensitive switch in our NFC circuit. As shown as Figure 3f, the different response levels may be related to the various protein levels contained in different meats, which determine the concentration of released amines.³¹

PTS-PAni was integrated into the NFC tag by an inkjet printing process, as discussed in our previous report, to realize an odor-sensitive switch function in the NFC tag.³² As an information-indicating terminal, the NFC tag can communicate passively with smartphones at 13.56 MHz and is powered wirelessly by generating a voltage across its antenna coil when receiving a radio frequency field emitted by mobile devices. Then, the tag resonates the same signal and transfers data back to the mobile device through load modulation.³ The readability of an NFC tag depends on whether its complex impedance matches the reading terminals. It is worth noting that the response of the NFC tag can be designed to be either “On-to-Off” (PAni is integrated in series with the circuit) or “Off-to-On” (PAni is integrated in parallel with the circuit) upon contact with chemicals.^{2,15} We chose the latter mode due to its compatibility with nondestructive printing technology and more selective working principle. Many factors can turn an On state to an Off state (i.e., NFC tag is damaged), but only more selective and rigid factors can turn an Off state to an On state. To fabricate an Off-to-On tag, we simply short the coils of the NFC tag directly by conductive PTS-PAni (Figure 2d). When low-resistance PAni is applied to the circuit, less signal resonates, as shown as Figure 4a. Then, the tag presents in the Off state and is unreadable because of the mismatch in the impedance of the NFC tag with the reader’s,³³ which corresponds to a reduced reflection coefficient (S_{11}). Herein, S_{11} is defined as

$$S_{11} = \lg \Gamma = \lg \left[\frac{Z_L - Z_0}{Z_L + Z_0} \right] \quad (2)$$

where Z_L and Z_0 represent the complex impedances of the tag and reader, respectively. A higher S_{11} indicates that more energy is absorbed by the NFC tag and the tag is more readable.² The tag will be reswitched to an On state upon contact with TVBN, which dedopes PAni to the insulating state and eliminates the direct short effect.

To investigate the quantitative relationship between PTS-PAni and S_{11} , we compared the S_{11} of the tag in parallel with different amounts of PTS-PAni, as shown as Figure 4a.¹⁵ Different numbers of dots of PTS-PAni were printed on the coil (Figure 2d). When the direct short effect was gradually introduced to the circuit, a relation between S_{11} and the amount of PTS-PAni was observed, indicating that the printed PTS-PAni is an effective way to switch S_{11} between unreadable (Off) and readable (On). The S_{11} -frequency relationship in parallel with fixed standard resistors modified into the tag in the same way was used as a control (Figure 4b). A lower resistance applied in the same way to the modified coil decreased the Z_L and S_{11} of the tag, in accordance with its definitional equation. The actual resonance frequency (f_0) remained constant with only a very slight offset (<1.5 MHz). This is consistent with the Thomson equation,

$$f_0 = \frac{1}{2\pi\sqrt{LC}} \quad (3)$$

where f_0 has no relation to the resistive elements.³⁴ The very small offset is caused by the actual manufacturing process but has been proven to be acceptable for consistent device performance. The quantitative relationship between the resonance strength and printed PAni dots is very useful to tune the response threshold of the tag toward TVBN.

The PANi resistance related to S_{11} enables switchable readability in the presence of TVBN. When the NFC tag was exposed to TVBN, the resistance of PTS–PANi rose sharply with such a high sensitivity that it results in a switch back to the readable status of the tag because the tag's impedance rematches with the reader's. We exposed the modified NFC tag to different concentrations of NH_3 (Figure 4c). The detection limit is 5 ppm, which corresponds to the initial decomposition of meat.¹³ The higher the concentration of NH_3 , the more the resistance of PTS–PANi increased, while that of S_{11} decreased. Notably, f_0 remained almost unchanged (top inset of Figure 4c). ΔS_{11} is positively and sensitively correlated to the NH_3 concentration. The dashed line in Figure 4c indicates the readout threshold of the tag. Once S_{11} exceeds the threshold, the NFC tag was switched on and sent signals back to the smartphone. The switching time reveals the concentration of amines and spoilage level. Higher concentrations of TVBN lead to greater and faster resistive changes and result in a short switching time, demonstrating that the sensitive PTS–PANi sensor is an ideal switch to use in an NFC tag for amine sensing. Note that the threshold line can be adjusted by controlling the direct short effect by the number of dots of PANi printed on the tag.

The PTS–PANi switch-integrated NFC tag can be used for practical applications of detecting meat spoilage. In daily life, lightly spoiled meat is not easily noticeable but indeed harmful to health, and a precise and low-cost badge for food spoilage detection via assistance of smartphones can be satisfying. As shown in Figure 4d, a badge was put in a container with a piece of spoiled meat, and a smartphone with NFC function can receive the signal to produce an alarm when the meat is spoiled (Supplemental Video). This process indicates that our switchable badge has potential in the detection of spoiled or spoiling food in daily life, storage, and supply chains.

In summary, we developed an easy-to-implement, sensitive wireless food sensor based on nanostructured conductive polymers for the convenient and low-cost detection of food spoilage with the following advantages: (a) PTS-doped and cross-linked PANi exhibits high sensitivity toward amines, for example, 46% and 17% sensitivity toward 5 ppm putrescine and cadaverine, respectively, and was proven to be a suitable switch material for NFC tags; (b) the printed PANi-modified NFC tag resulted in a complex impedance dependent on the integrated conductive polymer gas sensor, where the resistance of the conductive polymer directly switched the readability of the NFC tag; (c) the sensing material is compatible with inkjet printing technology, thus giving potential for the roll-to-roll fabrication of active NFC tags. We demonstrated smartphone-readable meat spoilage detection using the modified wireless badge and envision that such a switchable badge holds promise in the field of intelligent wireless detection and sensing.

■ ASSOCIATED CONTENT

Supporting Information

The Supporting Information is available free of charge on the ACS Publications website at DOI: 10.1021/acs.nanolett.8b01825.

Detailed experimental procedures, supplementary characterization and measurements of the PTS–PANi, and summary of sensing performances of polyaniline-based sensors (PDF)

Supplemental Video (MP4)

■ AUTHOR INFORMATION

Corresponding Authors

*E-mail: ljpan@nju.edu.cn.

*E-mail: yshi@nju.edu.cn.

*E-mail: ghyu@austin.utexas.edu.

ORCID

Lijia Pan: 0000-0002-8917-7843

Guihua Yu: 0000-0002-3253-0749

Author Contributions

Z.M. and P.C. contributed equally to this work. L.P., P.C., Z.M., and G.Y. designed the experiments, Z.M., P.C., and K.Y. worked on materials synthesis, device fabrication, and testing. The manuscript was written through contributions of all authors. All authors have given approval to the final version of the manuscript.

Notes

The authors declare no competing financial interest.

■ ACKNOWLEDGMENTS

L.P. and Y.S. would like to acknowledge the financial support of the National Key Research and Development program of China under Grant 2017YFA0206302, the National Natural Science Foundation of China under Grants 61674078, 61229401, 41401257, and 1157436, and the PAPD program. G.Y. acknowledges the financial support from Alfred P. Sloan Research Fellowship and Camille Dreyfus Teacher-Scholar Award.

■ REFERENCES

- (1) Kim, J.; Salvatore, G. A.; Araki, H.; Chiarelli, A. M.; Xie, Z.; Banks, A.; Sheng, X.; Liu, Y.; Lee, J. W.; Jang, K.-I. Battery-Free, Stretchable Optoelectronic Systems for Wireless Optical Characterization of the Skin. *Sci. Adv.* **2016**, *2* (8), e1600418.
- (2) Azzarelli, J. M.; Mirica, K. A.; Ravnsbæk, J. B.; Swager, T. M. Wireless Gas Detection with a Smartphone via Rf Communication. *Proc. Natl. Acad. Sci. U. S. A.* **2014**, *111* (51), 18162–18166.
- (3) Want, R. An Introduction to RFID Technology. *IEEE Pervasive Comput.* **2006**, *5* (1), 25–33.
- (4) Shalaby, A. R. Significance of Biogenic Amines to Food Safety and Human Health. *Food Res. Int.* **1996**, *29* (7), 675–690.
- (5) Naila, A.; Flint, S.; Fletcher, G.; Bremer, P.; Meerdink, G. Control of Biogenic Amines in Food—Existing and Emerging Approaches. *J. Food Sci.* **2010**, *75* (7), R139–R150.
- (6) Karovicova, J.; Kohajdova, Z. Biogenic Amines in Food. *Chem. Pap.* **2005**, *59* (1), 70–79.
- (7) Manetta, A. C.; Di Giuseppe, L.; Tofalo, R.; Martuscelli, M.; Schirone, M.; Giammarco, M.; Suzzi, G. Evaluation of Biogenic Amines in Wine: Determination by an Improved HPLC-PDA Method. *Food Control* **2016**, *62*, 351–356.
- (8) Carelli, D.; Centonze, D.; Palermo, C.; Quinto, M.; Rotunno, T. An Interference Free Amperometric Biosensor for the Detection of Biogenic Amines in Food Products. *Biosens. Bioelectron.* **2007**, *23* (5), 640–647.
- (9) Wang, Z.; Liu, F.; Lu, C. Evolution of Biogenic Amine Concentrations in Foods through Their Induced Chemiluminescence Inactivation of Layered Double Hydroxide Nanosheet Colloids. *Biosens. Bioelectron.* **2014**, *60*, 237–243.
- (10) Karpas, Z.; Tilman, B.; Gdalevsky, R.; Lorber, A. Determination of Volatile Biogenic Amines in Muscle Food Products by Ion Mobility Spectrometry. *Anal. Chim. Acta* **2002**, *463* (2), 155–163.
- (11) Liu, S. F.; Petty, A. R.; Sazama, G. T.; Swager, T. M. Single-Walled Carbon Nanotube/Metalloporphyrin Composites for the Chemiresistive Detection of Amines and Meat Spoilage. *Angew. Chem., Int. Ed.* **2015**, *54* (22), 6554–6557.

- (12) Fiddes, L. K.; Chang, J.; Yan, N. Electrochemical Detection of Biogenic Amines during Food Spoilage Using an Integrated Sensing RFID Tag. *Sens. Actuators, B* **2014**, *202*, 1298–1304.
- (13) Yamanaka, H.; Shiomi, K.; Kikuchi, T. Cadaverine as a Potential Index for Decomposition of Salmonoid Fishes. *Shokuhin Eiseigaku Zasshi* **1989**, *30* (2), 170–174.
- (14) Xu, G.; Zhang, Q.; Lu, Y.; Liu, L.; Ji, D.; Li, S.; Liu, Q. Passive and Wireless near Field Communication Tag Sensors for Biochemical Sensing with Smartphone. *Sens. Actuators, B* **2017**, *246*, 748–755.
- (15) Zhu, R.; Azzarelli, J. M.; Swager, T. M. Wireless Hazard Badges to Detect Nerve-Agent Simulants. *Angew. Chem., Int. Ed.* **2016**, *55* (33), 9662–9666.
- (16) Pan, L.; Yu, G.; Zhai, D.; Lee, H. R.; Zhao, W.; Liu, N.; Wang, H.; Tee, B. C.-K.; Shi, Y.; Cui, Y.; et al. Hierarchical Nanostructured Conducting Polymer Hydrogel with High Electrochemical Activity. *Proc. Natl. Acad. Sci. U. S. A.* **2012**, *109* (24), 9287–9292.
- (17) Wang, Y.; Shi, Y.; Pan, L.; Ding, Y.; Zhao, Y.; Li, Y.; Shi, Y.; Yu, G. Dopant-Enabled Supramolecular Approach for Controlled Synthesis of Nanostructured Conductive Polymer Hydrogels. *Nano Lett.* **2015**, *15* (11), 7736–7741.
- (18) Zhao, F.; Shi, Y.; Pan, L.; Yu, G. Multifunctional Nanostructured Conductive Polymer Gels: Synthesis, Properties, and Applications. *Acc. Chem. Res.* **2017**, *50* (7), 1734–1743.
- (19) Humpolicek, P.; Kasparkova, V.; Saha, P.; Stejskal, J. Biocompatibility of Polyaniline. *Synth. Met.* **2012**, *162* (7), 722–727.
- (20) Ramanathan, K.; Bangar, M. A.; Yun, M.; Chen, W.; Myung, N. V.; Mulchandani, A. Bioaffinity Sensing Using Biologically Functionalized Conducting-Polymer Nanowire. *J. Am. Chem. Soc.* **2005**, *127* (2), 496–497.
- (21) Sun, K.-H.; Liu, Z.; Liu, C.; Yu, T.; Shang, T.; Huang, C.; Zhou, M.; Liu, C.; Ran, F.; Li, Y.; et al. Evaluation of in Vitro and in Vivo Biocompatibility of a Myo-Inositol Hexakisphosphate Gelated Polyaniline Hydrogel in a Rat Model. *Sci. Rep.* **2016**, *6*, 23931.
- (22) CFR - Code of Federal Regulations Title 21,, the United States Food and Drug Administration (FDA), <https://www.accessdata.fda.gov/scripts/cdrh/cfdocs/cfcfr/cfrsearch.cfm?fr=175.105> (accessed Apr 22, 2018).
- (23) Li, L.; Wang, Y.; Pan, L.; Shi, Y.; Cheng, W.; Shi, Y.; Yu, G. A Nanostructured Conductive Hydrogels-Based Biosensor Platform for Human Metabolite Detection. *Nano Lett.* **2015**, *15* (2), 1146–1151.
- (24) Zhai, D.; Liu, B.; Shi, Y.; Pan, L.; Wang, Y.; Li, W.; Zhang, R.; Yu, G. Highly Sensitive Glucose Sensor Based on Pt Nanoparticle/Polyaniline Hydrogel Heterostructures. *ACS Nano* **2013**, *7* (4), 3540–3546.
- (25) Li, L.; Shi, Y.; Pan, L.; Shi, Y.; Yu, G. Rational Design and Applications of Conducting Polymer Hydrogels as Electrochemical Biosensors. *J. Mater. Chem. B* **2015**, *3* (15), 2920–2930.
- (26) Huang, J.; Virji, S.; Weiller, B. H.; Kaner, R. B. Polyaniline Nanofibers: Facile Synthesis and Chemical Sensors. *J. Am. Chem. Soc.* **2003**, *125* (2), 314–315.
- (27) Wang, Y.; Tran, H. D.; Liao, L.; Duan, X.; Kaner, R. B. Nanoscale Morphology, Dimensional Control, and Electrical Properties of Oligoanilines. *J. Am. Chem. Soc.* **2010**, *132* (30), 10365–10373.
- (28) Abdulla, S.; Mathew, T. L.; Pullithadathil, B. Highly Sensitive, Room Temperature Gas Sensor Based on Polyaniline-Multiwalled Carbon Nanotubes (PANI/MWCNTs) Nanocomposite for Trace-Level Ammonia Detection. *Sens. Actuators, B* **2015**, *221*, 1523–1534.
- (29) Bandgar, D. K.; Navale, S. T.; Nalage, S. R.; Mane, R. S.; Stadler, F. J.; Aswal, D. K.; Gupta, S. K.; Patil, V. B. Simple and Low-Temperature Polyaniline-Based Flexible Ammonia Sensor: A Step towards Laboratory Synthesis to Economical Device Design. *J. Mater. Chem. C* **2015**, *3* (36), 9461–9468.
- (30) Tian, J.; Yang, G.; Jiang, D.; Su, F.; Zhang, Z. A Hybrid Material Consisting of Bulk-Reduced TiO₂, Graphene Oxide and Polyaniline for Resistance Based Sensing of Gaseous Ammonia at Room Temperature. *Microchim. Acta* **2016**, *183* (11), 2871–2878.
- (31) Hu, Y.; Ma, X.; Zhang, Y.; Che, Y.; Zhao, J. Detection of Amines with Fluorescent Nanotubes: Applications in the Assessment of Meat Spoilage. *ACS Sens.* **2016**, *1* (1), 22–25.
- (32) Li, L.; Pan, L.; Ma, Z.; Yan, K.; Cheng, W.; Shi, Y.; Yu, G. All Inkjet-Printed Amperometric Multiplexed Biosensors Based on Nanostructured Conductive Hydrogel Electrodes. *Nano Lett.* **2018**, *18*, 3322.
- (33) Potyralo, R. A.; Nagraj, N.; Tang, Z.; Mondello, F. J.; Surman, C.; Morris, W. Battery-Free Radio Frequency Identification (RFID) Sensors for Food Quality and Safety. *J. Agric. Food Chem.* **2012**, *60* (35), 8535–8543.
- (34) Park, J.; Kim, J.; Kim, K.; Kim, S.-Y.; Cheong, W. H.; Park, K.; Song, J. H.; Namgoong, G.; Kim, J. J.; Heo, J.; et al. Wearable, Wireless Gas Sensors Using Highly Stretchable and Transparent Structures of Nanowires and Graphene. *Nanoscale* **2016**, *8* (20), 10591–10597.